Covalent Linkage of Prosthetic Heme to CYP4 Family P450 Enzymes†

Kirk R. Henne,‡ Kent L. Kunze,‡ Yi-Min Zheng,‡ Peter Christmas,§ Roy J. Soberman,§ and Allan E. Rettie*,‡

Department of Medicinal Chemistry, School of Pharmacy, University of Washington, Seattle, Washington 98195, and Center for Immunology and Inflammatory Disease, Massachusetts General Hospital and Harvard Medical School, Charlestown, Massachusetts 02129

Received June 6, 2001; Revised Manuscript Received August 23, 2001

ABSTRACT: An extensive body of research on the structural properties of cytochrome P450 enzymes has established that these proteins possess a *b*-type heme prosthetic group which is noncovalently bound at the active site. Coordinate, electrostatic, and hydrogen bond interactions between the protein backbone and heme functional groups are readily overcome upon mild acid treatment of the enzyme, which releases free heme from the protein. In the present study, we have used a combination of HPLC, LC/ESI-MS, and SDS−PAGE techniques to demonstrate that members of the mammalian CYP4B, CYP4F, and CYP4A subfamilies bind their heme in an unusually tight manner. HPLC chromatography of CYP4B1 on a POROS R2 column under mild acidic conditions caused dissociation of less than one-third of the heme from the protein. Moreover, heme was not substantially removed from CYP4B1 under electrospray or electrophoresis conditions that readily release the prosthetic group from other non-CYP4 P450 isoforms. This was evidenced by an intact protein mass value of 59 217 ± 3 amu for CYP4B1 (i.e., apoprotein plus heme) and extensive staining of this ∼60 kDa protein with tetramethylbenzidine/H_2O_2 following SDS−PAGE. In addition, treatment of CYP4B1, CYP4F3, and CYP4A5/7 with strong base generated a new, chromatographically distinct, polar heme species with a mass of 632.3 amu rather than 616.2 amu. This mass shift is indicative of the incorporation of an oxygen atom into the heme nucleus and is consistent with the presence of a novel covalent ester linkage between the protein backbone of the CYP4 family of mammalian P450s and their heme catalytic center.

Cytochrome P450 (CYP)[1] enzymes are a superfamily of heme-containing monooxygenases capable of oxidizing a wide array of environmentally encountered xenobiotics and endogenous biological modulators (*1*−*3*). The ubiquitous presence of P450s throughout the animal and plant kingdoms and their impressive catalytic versatility have spawned widespread research efforts to elucidate structure−function relationships among the protein products of more than 200 gene families so far identified (http://drnelson.utmem.edu/CytochromeP450.html).

All P450 isoforms possess a common heme cofactor (iron protoporphyrin IX) that is required for oxygen binding and formation of the active oxidant species. The heme iron center is buried in the interior of the protein, and substrate access is limited in part by the dimensions of the active site channel, as exemplified by the crystal structure for substrate-bound CYP102 (*4*). In the case of CYP101, the heme is so deeply buried in the protein that diffraction data do not reveal a probable path for the natural camphor substrate to access the enzyme active site (*5*). Nonetheless, mild acidification releases the heme cofactor from both soluble and membrane-bound P450s, and this can be rationalized on the basis of the noncovalent nature of the interactions that bind heme to these P450s. From the standpoint of function, the most important interaction is the coordinate bond between a completely conserved cysteine residue that serves as the proximal ligand to the iron atom (*6*). The S−Fe bond is a defining characteristic of P450 proteins that gives rise to their unique spectroscopic UV absorbance at 450 nm upon reduction and binding of carbon monoxide (*7*). Aside from the cysteine thiolate bond, heme binding in P450 enzymes is facilitated via other noncovalent interactions between protein and heme functional groups. Crystal structures of several bacterial P450s (*5*, *8*−*10*) and, most recently, a mammalian P450 (*11*) highlight the role of electrostatic interactions and hydrogen bonding to the negatively charged heme propionate groups. In addition, there is growing evidence that charged amino acids in the meander region also play a role in heme binding (*6*, *12*).

In a recent study of the topographical features of the CYP4B1 active site we found that, compared to well-characterized P450 enzymes such as CYP102 and CYP2B1, removal of the heme prosthetic group from acidified samples of rabbit CYP4B1 was a low-yield process (*13*). In the

† This investigation was supported by Grants GM49054 (A.E.R.) and GM61823 (R.J.S.) and DK59991 (P.C.) from the National Institutes of Health (NIH). Additional funding was provided by a grant from the Jewish Communal Fund (R.J.S.). K.R.H. was supported by NIH Training Grant GM07750.

* To whom correspondence should be sent at the Department of Medicinal Chemistry, Box 357610, University of Washington, Seattle, WA 98195. Telephone: (206) 685-0615. Fax: (206) 685-3252. E-mail: rettie@u.washington.edu.

‡ University of Washington.

§ Massachusetts General Hospital and Harvard Medical School.

[1] Abbreviations: CYP, cytochrome P450; HPLC, high-pressure liquid chromatography; LC/ESI-MS, liquid chromatography/electrospray ionization−mass spectrometry; amu, atomic mass units; SDS−PAGE, sodium dodecyl sulfate−polyacrylamide gel electrophoresis; TMBZ, 3,3′,5,5′-tetramethylbenzidine; DTT, dithiothreitol; βME, β-mercaptoethanol; PMSF, phenylmethanesulfonyl fluoride.

10.1021/bi011171z CCC: $20.00
Published on Web 10/03/2001

present study, HPLC, LC/ESI-MS, and SDS−PAGE techniques have been utilized to demonstrate that the heme group is held unusually tightly in the active site of rabbit CYP4B1. Base treatment of CYP4B1, as well as members of the rabbit CYP4A and human CYP4F subfamilies, releases a polar heme derivative which has incorporated an additional 16 amu. This is consistent with the presence of a *covalent* interaction between an acidic residue of these CYP4 proteins and the heme cofactor, similar to that noted recently for several rat CYP4A proteins (*14*). Therefore, the present study indicates that covalently linked heme may be a general structural phenomenon for mammalian CYP4 proteins.

EXPERIMENTAL PROCEDURES

Chemicals. ProtoGel acrylamide (30% w/v) was purchased from National Diagnostics (Atlanta, GA). Sucrose, DTT, and hemin chloride were from Sigma (St. Louis, MO). Trifluoroacetic acid (TFA) was from Pierce (Rockford, IL), and 3,3′,5,5′-tetramethylbenzidine (TMBZ) was obtained from Aldrich (Milwaukee, WI). Acetonitrile (Optima grade) and hydrogen peroxide were purchased from Fisher Scientific (Pittsburgh, PA).

Expression and Purification of CYP2C9, CYP4B1, and CYP4A5/7 Enzymes. Baculovirus expression and purification of human CYP2C9 were carried out as previously reported (*15*). Similarly, rabbit CYP4B1 was expressed in the baculovirus expression vector system and purified according to published procedures (*16*). The CYP4A5/7 protein mix isolated from untreated rabbit kidney cortex (*17*) was a generous gift from Drs. Dennis Koop and Ron Laetham (Oregon Health Sciences University, Portland, OR).

Expression and Purification of CYP4F3B. The *CYP4F3B* gene was obtained as previously described (*18*). To facilitate purification of CYP4F3B, a hexahistidine tag was added at the C-terminus of the CYP4F3B cDNA using PCR with the following primers: 5′-ATG CCA CAG CTG AGC CTG TCC TCG C-3′ and 5′-TCA GTG ATG GTG ATG GTG ATG GCT CAG GGG-3′. The PCR reaction was performed using pfu turbo DNA polymerase (Stratagene, Inc., La Jolla, CA) under the following conditions: 94 °C for 1 min, 45 °C for 1 min, 72 °C for 2 min, 30 cycles, followed by a cycle at 72 °C for 10 min. A 1.6 kb PCR product was cloned into a pCR2.1 vector and subsequently subcloned into the pFBacI baculovirus expression vector (Life Technologies, Rockville, MD) utilizing *Eco*RI restriction sites. The sequence of the target gene was confirmed by dye termination DNA sequencing.

CYP4F3B was expressed in insect cells according to methods described previously (*12*) using Ex-Cell 405 media (JRH Biosciences, Lenexa, KS) supplemented with 5% TC-100 media, 0.5% fetal bovine serum, penicillin G (10 000 units), streptomycin (10 μg/mL), and amphotericin B (25 μg/mL). Cells were harvested by centrifugation at 8000*g* for 20 min and resuspended in 100 mM potassium phosphate, 20% glycerol, 1% cholate, 1 mM EDTA, 0.2 mM PMSF, and 1 mM DTT, pH 7.4. The homogenized cells were stirred on ice for 30 min and centrifuged at 100000*g* for 40 min, and the supernatant was loaded directly onto an octyl-Sepharose column equilibrated with 10 mM potassium phosphate, 20% glycerol, 0.5% cholate, 1 mM DTT, 1 mM EDTA, and 0.2 mM PMSF, pH 7.4. CYP4F3B was eluted with buffer containing 10 mM potassium phosphate, 20% glycerol, 0.2% cholate, 1% Emulgen 911, 0.2 mM PMSF, and 0.1 mM DTT, pH 7.4, and dialyzed against 50 mM potassium phosphate containing 20% glycerol. The dialyzed enzyme was applied to an Ni-NTA column equilibrated with 50 mM potassium phosphate, 20% glycerol, 1 mM PMSF, 1% Emulgen 911, and 20 mM βME, pH 7.4. Following two washes with buffer A (50 mM potassium phosphate, 20% glycerol, 1 mM PMSF, 2 mM CHAPS, 0.5 M NaCl, and 20 mM βME, pH 7.4) supplemented sequentially with 5 mM imidazole and then 80 mM imidazole, the enzyme was eluted with 200 mM imidazole. The highly purified CYP4F3B preparation was dialyzed against 3 L of 100 mM potassium phosphate buffer containing 20% glycerol and 0.1 mM EDTA, pH 7.4, and stored at −70 °C until use.

HPLC−UV and LC/ESI-MS Instrumentation. HPLC−UV analysis was performed on a Shimadzu HPLC consisting of two LC-10ADvp pumps, an SPD-10Avp UV−vis detector, an SCL-10Avp controller, and a Rheodyne injector (Shimadzu Scientific Instruments, Inc., Columbia, MD; Rheodyne, Inc., Cotati, CA). During analysis, data were collected using PowerChrom software (version 2.1.3, ADInstruments, Ltd., Castle Hill, NSW, Australia) running on an Apple Power Macintosh 6100 computer. LC/ESI-MS analysis was performed using a Micromass Quattro II tandem quadrupole mass spectrometer (Micromass, Ltd., Manchester, U.K.) coupled to a Shimadzu LC instrument identical to that described above except for the addition of an SIL-10ADvp auto injector. The mass spectrometer was run in electrospray ionization mode (ESI) at a cone voltage of 45−55 V, source block temperature of 100 °C, and a desolvation temperature of 350 °C. Data analysis was carried out using Windows NT based Micromass MassLynxNT 3.2 and MaxEnt software.

HPLC−UV and LC/ESI-MS Sample Preparation and Analysis. Proteins were injected on LC columns in either storage buffer (100 mM potassium phosphate, 0.1 mM EDTA, and 20% glycerol, pH 7.4) or sucrose/Tris buffer (250 mM sucrose, 50 mM Tris, and 1 mM EDTA, pH 8.0). In cases where removal of glycerol aided analysis, exchange into the sucrose/Tris was performed with Bio-Spin Bio-Gel P-6 columns (Bio-Rad, Hercules, CA) according to the manufacturer's protocol. Denaturation of CYP4B1 prior to HPLC analysis was accomplished by exposure to urea and DTT. A 100 μL aliquot (400 pmol) of CYP4B1 was first exchanged into sucrose/Tris buffer before being supplemented with 180 μL of denaturation buffer (8 M urea in 0.4 M ammonium bicarbonate) and 20 μL of 45 mM DTT. The mixture (300 μL total volume) was then heated for 15 min at 50 °C before injection onto the column. Heme was dissociated from the CYP4B1 holoenzyme by treatment with sodium hydroxide. Enzyme aliquots in storage buffer were mixed 1:1 with a freshly prepared 0.5 M sodium hydroxide solution and left to sit on ice for 10−20 min. Loss of the heme moiety from CYP4 proteins was monitored by following absorbance of HPLC eluates at both 214 and 400 nm. LC analysis of P450 proteins was performed on a self-packed 2.1 × 150 mm narrow bore POROS R2 column (Applied Biosystems, Foster City, CA). The mobile phase used in conjunction with the R2 packing consisted of 0.05% TFA (A) and acetonitrile containing 0.05% TFA (B). Initially, the flow rate was set at 1 mL/min with a solvent

composition of 20% B. At 3 min, total flow was adjusted to 0.2 mL/min for the purposes of LC-MS compatibility, and a linear gradient was established that increased from 20% B to 85% B over 20 min. Under these conditions, polar heme eluted at ~10 min, free heme at ~12 min and P450 proteins eluted between 14 and 16 min.

Protein Gel Electrophoresis and Heme/Protein Staining. SDS−PAGE was performed using a Bio-Rad Mini-Protean II apparatus. To facilitate in-gel detection of free or P450 associated heme, the method of Thomas et al. was utilized, with minor modifications (*19*). Briefly, 9% resolving gels were preelectrophoresed at 10 °C overnight at low voltage to remove excess ammonium persulfate. Samples were boiled for 5 min in buffer containing 7% SDS prior to loading. The use of DTT or other thiol-containing agents was explicitly avoided due to their propensity to react with heme (*19*−*23*) and potentially interfere with the heme peroxidase activity necessary for staining (*24*, *25*). Electrophoresis was carried out in fresh buffer over the course of 2−3 h at 10 °C. To stain gels for heme detection, a 1.5 mg/mL solution of TMBZ was freshly prepared in methanol. After the TMBZ dissolved fully, 3 parts of the resulting solution were mixed with 7 parts of 250 mM sodium acetate buffer (pH 5.0). Gels were immersed in this mixture for 1−2 h in the dark before the addition of hydrogen peroxide to a final concentration of 30 mM. Over the next 30 min, light blue bands emerged, indicating the presence of heme. Photographs were taken immediately after the gels were developed as the staining intensity eventually diminishes due to light sensitivity. Short-term storage of stained gels could be achieved in 1:2:17 glacial acetic acid/2-propanol/water. Staining of gels for protein content was carried out with Coomassie R250 dye using standard procedures. Protein samples for Coomassie gels were treated identically to those for TMBZ staining so that results from the different staining techniques could be compared directly.

Spectroscopic Characterization of CYP Proteins. P450 measurements (reduced-CO complex vs reduced enzyme) were taken with a Shimadzu UV-2401PC spectrophotometer (Shimadzu Scientific Instruments, Inc., Columbia, MD) using the method of Estabrook et al. (*26*). Pyridine hemochromes were characterized as previously described (*27*).

RESULTS

HPLC−UV Analysis of P450 Proteins. Chromatography of CYP2C9 on a POROS R2 stationary phase under mild acidic conditions resolves this P450 enzyme into two components: free heme that elutes at 11.8 min and apoprotein that elutes at 15.6 min (Figure 1A). The observation that CYP2C9 completely loses its heme upon exposure to acetonitrile/water/TFA during HPLC analysis is consistent with previous reports (*28*). In contrast, CYP4B1 appears to retain a substantial portion of its heme when chromatographed under these conditions, as evidenced by the pronounced absorbance at 400 nm of the protein peak eluting at 13.9 min (Figure 1B).

Several procedures were investigated in attempts to dissociate the remainder of the enzyme-bound heme in CYP4B1. Samples denatured by means of urea/DTT/heat treatment prior to HPLC analysis were chromatographically indistinguishable from the "native" enzyme experiments depicted in Figure 1B (data not shown). However, when CYP4B1 samples were pretreated with an equal volume of 0.5 M NaOH for 10−20 min at 0 °C before analysis, a new, chromatographically distinct "polar" heme species appeared with a retention time of 10.3 min (Figure 1C).

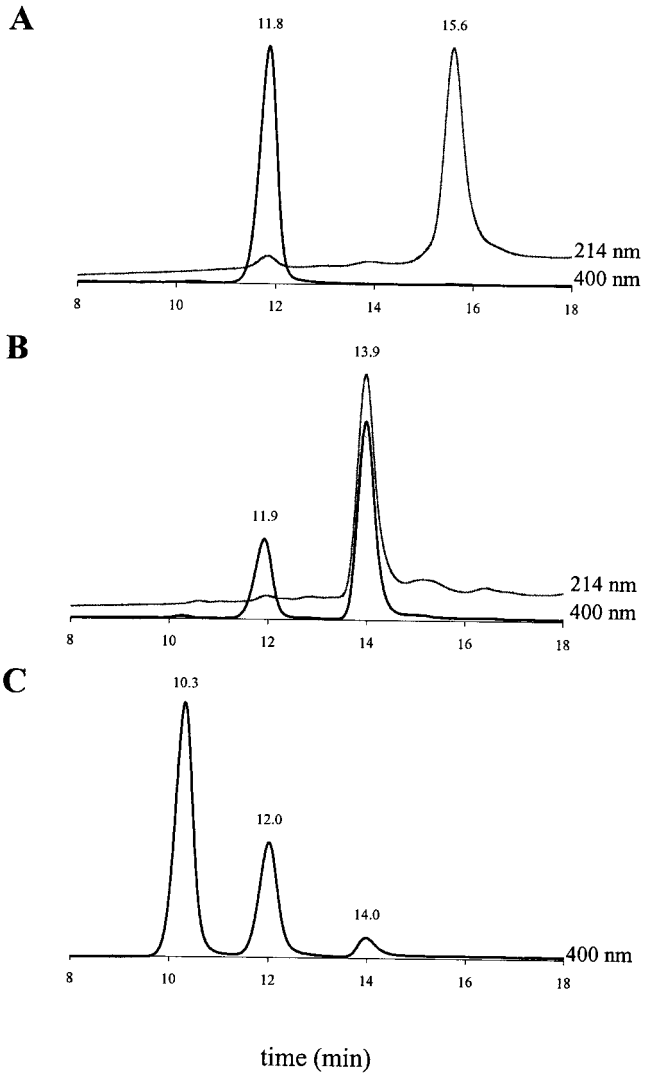

FIGURE 1: POROS R2 chromatography of CYP2C9 and CYP4B1. Panel A: HPLC−UV analysis of CYP2C9 with detection at 214 nm (upper trace) and 400 nm (lower trace). Apo-CYP2C9 elutes at 15.6 min, and free heme elutes at 11.8 min. Panel B: HPLC−UV analysis of CYP4B1. Heme-associated CYP4B1 elutes at 13.9 min, and free heme elutes at 11.9 min. Panel C: HPLC−UV analysis of CYP4B1 after pretreatment with NaOH. The new peak at 10.3 min is an unexpected polar heme species not detected in experiments with CYP2C9.

LC/ESI-MS Analysis of CYP2C9 and CYP4B1 Proteins. Electrospray mass spectrometry analysis of the CYP2C9 protein peak obtained in Figure 1A yielded an $(M + H)^+$ value for the intact protein of 55 630 ± 4 amu ($n = 3$). A typical result for this enzyme is shown in Figure 2A. The theoretical average mass for the CYP2C9 apoprotein, based on the primary amino acid sequence in the SwissProt database, is 55 629 amu. These data confirm the facile loss of the heme prosthetic group from CYP2C9. The experimentally determined mass of CYP4B1 following column chromatography is 59 217 ± 3 amu ($n = 13$) (Figure 2B). This is an increase of some 612 mass units relative to the value of 58 605 amu predicted from the primary sequence

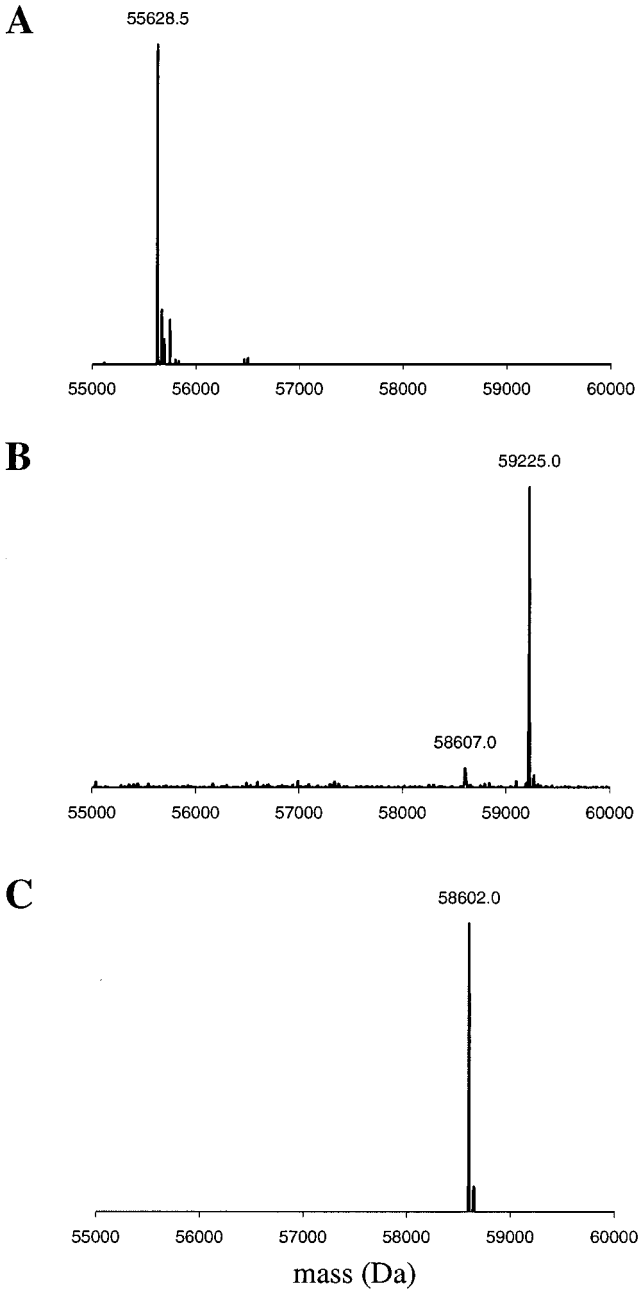

FIGURE 2: LC/ESI-MS analysis of intact CYP2C9 and CYP4B1. Panel A: A deconvoluted mass spectrum depicting the experimentally determined mass of CYP2C9 at 55 629 amu. Panel B: The deconvoluted mass spectrum of CYP4B1. The mass at 59 225 is indicative of CYP4B1 holoenzyme, while the minor peak at 58 607 represents apo-CYP4B1. Panel C: The deconvoluted mass spectrum of CYP4B1 after exposure to NaOH, demonstrating complete conversion to apo-CYP4B1.

of the apoenzyme and obtained experimentally for the base-treated protein (Figure 2C). These data confirm that a significant portion of the heme remains bound to CYP4B1 under either acidic or electrospray conditions.

SDS−PAGE Analysis of CYP2C9 and CYP4B1. It is well recognized that conventional electrophoresis conditions result in the nearly complete dissociation of heme from P450 holoprotein. Therefore, to provide an independent evaluation of the nature of the heme−P450 interaction in CYP4B1, we conducted SDS−PAGE analysis with TMBZ/hydrogen peroxide staining specifically for detection of the heme group (Figure 3, right panel). Intense staining in the 55 kDa region

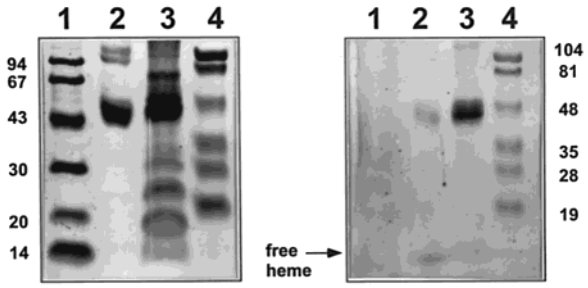

FIGURE 3: Differentially stained SDS−PAGE protein gels showing the analysis of CYP2C9 and CYP4B1 enzymes. Left panel: Protein gel stained with Coomassie dye. Lanes: 1, molecular weight markers; 2, 40 pmol of CYP2C9; 3, 40 pmol of CYP4B1; 4, prestained molecular weight markers. Right panel: Protein gel developed with TMBZ/hydrogen peroxide stain specific for heme. The contents of lanes 1−4 are identical to the gel pictured in the left panel. A faint band corresponding to free heme can be seen near the dye front in lane 2, as indicated by the arrow.

is evident only for the CYP4B1 preparation, whereas marked staining is evident for free heme only at the dye front of CYP2C9. A Coomassie-stained gel of these two proteins (Figure 3, left panel) confirmed that similar amounts of P450 were loaded in each lane and demonstrated that the lack of DTT in the P450 lanes is responsible for smearing of the protein bands.

LC/ESI-MS Analysis of Heme Released from CYP2C9 and CYP4B1 Proteins. Mass analysis of the free heme generated from CYP2C9 provided the spectrum shown in Figure 4A. The signal at *m*/*z* 616 corresponds to the expected molecular ion for heme, while the peak at *m*/*z* 657 represents heme adducted with acetonitrile from the HPLC solvent. Similar heme−solvent adducts have been reported previously with both acetonitrile and methanol (*29*). Because similar LC/ESI-MS experiments analyzing the protoporphyrin IX standard did not produce such an adduct, the presence of the iron atom in the heme appears necessary for solvent adduction (data not shown). The peak at *m*/*z* 557 appears to arise from the loss of 59 amu ($-CH_2COOH$) from one of the propionate side chains. While heme fragmentation of this type occurs readily under EI conditions (*30*), information regarding similar in-source fragmentation of heme under ESI conditions is not widely available. Figure 4B represents heme from the native CYP4B1 enzyme which, as expected, exhibits a mass spectrum identical to that of the heme released from CYP2C9. Most interestingly, the new heme product (10.3 min peak in Figure 1C) arising from base treatment of CYP4B1 produced a mass spectrum with all three of the peaks shifted to higher mass by 16 amu (Figure 4C). This indicates incorporation of one oxygen atom into the iron protoporphyrin IX structure and is consistent with the observed decrease in retention time expected for a more polar hydroxy heme species. Base-catalyzed formation of a monohydroxy heme derivative implies a novel covalent ester linkage between CYP4B1 apoprotein and the heme prosthetic group, as reported recently for several rat CYP4A enzymes (*14*).

Heme Binding Characteristics in Members of Other CYP4 Subfamilies. To investigate whether covalently linked hemes are broadly characteristic of mammalian CYP4 isoforms, members of the rabbit CYP4A and human CYP4F subfamilies were subjected to base treatment and chromatographic analysis. Both the CYP4A5/7 mixture and human CYP4F3B

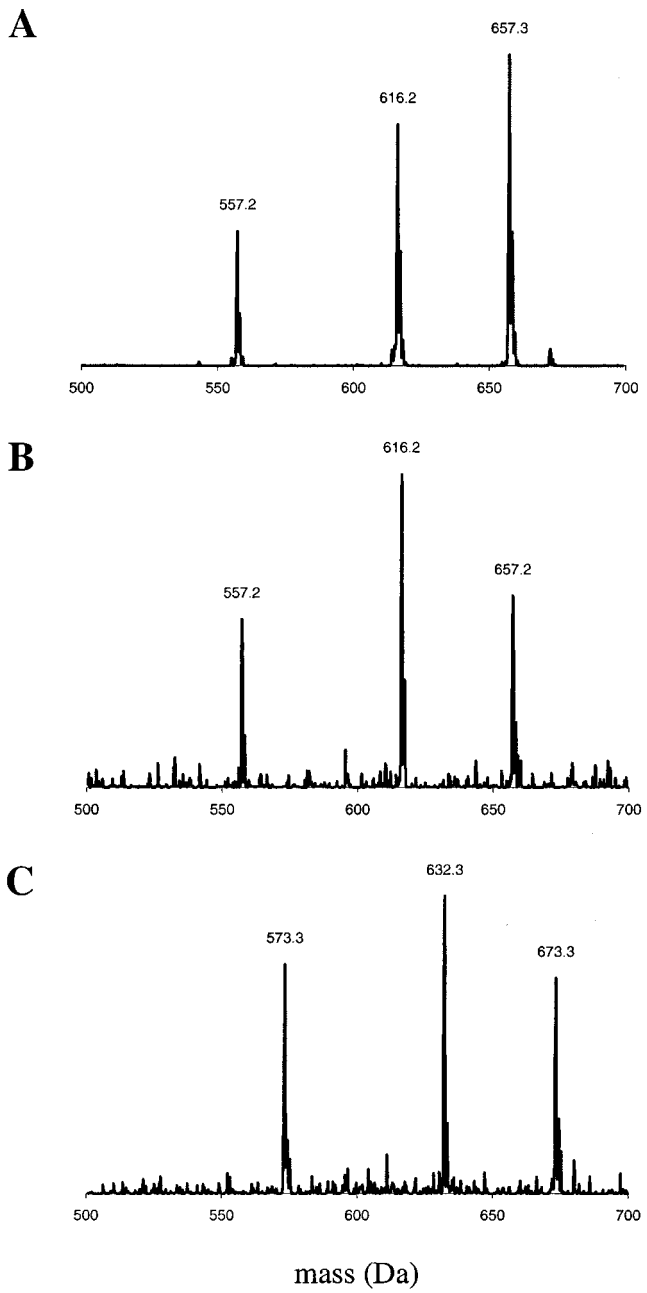

FIGURE 4: LC/ESI-MS analysis of heme extracted from CYP2C9 and CYP4B. Panel A: Mass spectrum of the free heme from CYP2C9. The molecular ion for the heme is 616 amu. The signals at *m*/*z* 657 and 557 represent a heme−acetonitrile adduct and a heme fragment, respectively. Panel B: Mass spectrum of the minor free heme component that readily dissociates from CYP4B1. Panel C: Mass spectrum of the major, modified polar heme fraction from CYP4B1, demonstrating the addition of 16 amu.

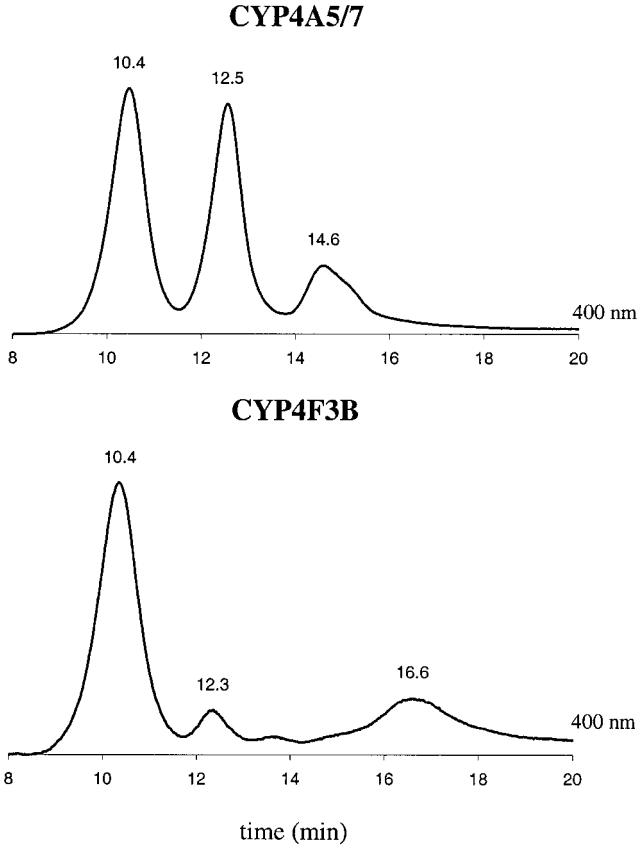

FIGURE 5: HPLC−UV analysis of CYP4A5/7 and CYP4F3B. Upper panel: CYP4A5/7 after pretreatment with base. Lower panel: CYP4F3B after pretreatment with base. Note the appearance of the monohydroxy heme species at a retention time of 10.4 min.

Table 1: Covalent Heme Binding and Spectral Properties of Selected CYP Enzymes

CYP enzyme	% heme covalently bound[a]	CO binding spectrum λ_{max} (nm)	pyridine hemochrome α-band, β-band (nm)
CYP2C9	<1	450	556, 525
CYP4B1	74	448	557, 525
CYP4A5/7	60	451	557, 526
CYP4F3B	80	449	557, 525

[a] As determined by LC−UV at 400 nm and given as the mean of three determinations.

generated a new polar heme species (Figure 5), and mass spectrometry analysis confirmed the monohydroxy modification (data not shown).

Spectral Studies of Selected CYP Enzymes. The ratio of absorbance at 400 nm for free heme relative to the holoprotein provides an estimate of the percentage of heme that is covalently bound to P450. For CYP4B1, CYP4A5/7, and CYP4F3B this value is 60−80%, whereas for CYP2C9 it is <1% (Table 1). Table 1 also summarizes the spectral properties of CYP2C9, CYP4B1, CYP4A5/7, and CYP4F3B with respect to CO binding and pyridine hemochromagens. The λ_{max} of the reduced CO complexes for all four enzymes is typical of P450 monooxygenases in general, regardless of the presence or absence of covalent heme binding. Similarly, the pyridine hemochromagens of the CYP4 enzymes exhibit α- and β-bands at wavelengths similar to those of CYP2C9 and consistent with other *b*-type hemes at ~557 and ~525 nm, respectively. Therefore, the presumptive covalent ester link in the mammalian CYP4 enzymes does not significantly alter the electronic absorbance spectrum in this region. This may help to explain why this unusual mode of heme attachment has not been noted earlier.

DISCUSSION

The heme prosthetic group of CYP enzymes is critical in P450-catalyzed oxidation reactions in order to bind molecular oxygen and form the active oxene species. Due to the importance of the heme moiety to enzyme function, the nature of the heme−protein interaction has been extensively

characterized, particularly in the case of the soluble isoforms. For bacterial P450s amenable to crystallization and X-ray diffraction (*5*, *6*, *8*, *9*), a completely conserved cysteine residue located in the "heme binding loop" provides the thiolate that coordinates with the heme iron. This axial cysteine ligand not only serves to help bind the heme in the active site but also has been implicated mechanistically in the O−O bond scission event that generates the perferryl species (*31*). Additional noncovalent contacts in bacterial P450s have been observed between the heme propionate side chains and amino acid residues located in the C-helix and β-strand 1−4 regions of the protein (*32*). Mammalian P450 isoforms are generally thought to bind heme in a manner similar to that of their bacterial counterparts. X-ray data gathered from a modified CYP2C5 enzyme show protein−heme contact points between the conserved cysteine and heme iron atom as well as between helix C and β-sheet 1−4 and the heme propionate side chains (*11*)—nearly identical to the bacterial enzymes. Such a finding legitimizes the notion that the heme binding regions of P450s are generally conserved across enzymes regardless of their biological source. Indeed, in the present study, the characteristics of heme binding to CYP2C9 examined by various techniques matched expectations based on both the enzyme's homology to CYP2C5 and the weight of historical data that has demonstrated repeatedly that P450−heme interactions are highly vulnerable to acidic conditions (*33*−*37*).

Although rabbit CYP4B1 is functionally rather unusual in its ability to ω-hydroxylate linear alkanes (*38*), there is no reason to expect a priori that the nature of the heme−protein interaction would differ substantively from that established for other P450s. However, HPLC, SDS−PAGE, and mass spectrometric analysis clearly demonstrate an unusually tight association between CYP4B1 and its heme cofactor relative to the CYP2C9 control. A plausible explanation for the unusually stable interaction between CYP4B1 and its heme could be the unexpected formation of an ester or amide linkage between an amino acid side chain from the protein (serine, threonine, lysine, etc.) and a propionate functionality of the heme. However, formation of an amide or ester with a protein residue would result in the loss of water (18 amu) from the adducted protein. That would mean that the predicted mass of the holoenzyme would be 59 203 Da instead of 59 221 Da. Because the mass accuracy of the instrument used is typically within 0.01%, a protein with a molecular mass of 60 kDa should have a measured mass within 6 mass units of the true value. The experimental holoenzyme mass of 59 217 Da for CYP4B1 is within the 6 mass unit error margin of 59 221 but well outside the expected margin of error for a protein with a mass of 59 203 Da. Furthermore, hydrolysis of such an ester/amide linkage by NaOH would free the heme in its native form, restoring the propionate and the putative amino acid side chain. The structure of the free heme liberated in this fashion would be unchanged, as would its mobility on the R2 column. Since the heme cofactor released from CYP4B1 by NaOH possesses an additional 16 amu and exhibits a decreased retention time on the column, the propionate ester/amide scenario is untenable.

A more likely explanation for the apparent covalent interaction and mass increase in heme removed from CYP4B1 by hydrolysis can be found by considering heme−protein interactions that have been characterized for myeloperoxidase (MPO) and lactoperoxidase (LPO). While these enzymes differ from P450s in that the axial ligand to heme is histidine, the catalytic cycles of the two enzymes are thought to be very similar (*39*). In the case of MPO (*40*) and LPO (*29*), structures for covalently bound hemes determined from X-ray and NMR studies, respectively, reveal ester linkages between heme methyl carbons and protein via backbone aspartate and glutamate residues. An autocatalytic mechanism leading to covalent attachment has been proposed, wherein heme methyl groups are oxidized by the enzyme during nonproductive turnover events to cationic species that are captured by appropriately positioned carboxylate groups (*41*). Moreover, heme that is removed from LPO by exhaustive proteolysis exhibited a mass of 648 amu, implying the incorporation of two oxygen atoms and the presence of two ester linkages. By HPLC, dihydroxy LPO-derived heme also exhibited an increase in polarity, similar to that seen in the present study for heme released from CYP4B1 by base. The analogous reaction in the case of CYP4B1, however, would need to occur at only one of the two heme methyl groups in order to account for the increase in 16 amu determined for CYP4B1's polar heme.

A very recent report published during our experiments with the CYP4B1 enzyme describes the covalent binding of heme to several rat and human CYP4A isoforms (*14*). Detailed analysis of peptides released from CYP4A3 by Pronase treatment favored glutamate-318 as the likely site of heme attachment in this and perhaps other CYP4A enzymes. Sequence alignments in the putative I-helix region of the

Table 2: Partial I-Helix Sequence Alignment of Various CYP Enzymes

CYP Enzyme [a]	Partial I-Helix Sequence
CYP102 (*B. megaterium*)	I T F L I ^{264}**A** G H E T T S
CYP1A2	N D I F G ^{317}**A** G F D T V T
CYP2A6	L N L F I ^{301}**G** G T E T V S
CYP2B6	L S L F F ^{298}**A** G T E T T S
CYP2C9	V D L F G ^{297}**A** G T E T T S
CYP2D6	A D L F S ^{305}**A** G M V T T S
CYP2E1	A D L F F ^{299}**A** G T E T T S
CYP3A4	I I F I F ^{305}**A** G Y E T T S
CYP4A3 (rat)	D T F M F ^{318}**E** G H D T T A
CYP4A5 (rabbit)	D T F M F ^{322}**E** G H D T T A
CYP4A7 (rabbit)	D T F M F ^{322}**E** G H D T T A
CYP4B1 (rabbit)	D T F M F ^{310}**E** G H D T T T
CYP4B1	D T F M F ^{315}**E** G H D T T T
CYP4F2	D T F M F ^{328}**E** G H D T T A
CYP4F3	D T F M F ^{328}**E** G H D T T A

[a] All sequences are for human enzymes unless otherwise noted.

rat CYP4A proteins, CYP4B1, CYP4A5/7, CYP4F2, and CYP4F3 (Table 2), demonstrate that all of these enzymes possess a glutamic acid residue at the same position, but as might be expected, representative members of CYP families 1−3, for which there is no evidence for covalent heme attachment, lack an acidic residue at this position. Since our experimental data show that base treatment also releases a monohydroxy heme species from CYP4A5/7 and CYP4F3B, covalent heme linkage may be a fairly general characteristic of the mammalian CYP4 family of enzymes.

In the present studies, the maximal degree of covalent binding of heme to CYP4 proteins was 80%, and so a major question remains about the catalytic competency of P450s that incorporate this base-labile ester linkage. Interestingly, an alignment of 57 human P450 sequences (http://drnelson.utmem.edu/humP450.aln.html) reveals that three CYP4 proteins, CYP4A20, CYP4F8, and CYP4F12, lack a carboxylate-containing residue at this position. Although no functional data are yet available for CYP4A20, preliminary catalytic data suggest that CYP4F8 and CYP4F12 have substrate specificities that are distinct from other CYP4F proteins (*42*, *43*). Therefore, it is tempting to speculate that heme adduction, by restricting the conformational flexibility in the P450 active site, might play an important role in contributing to the ω-hydroxylase specificity of the more "typical" CYP4 isoforms for both endogenous and exogenous substrates.

REFERENCES

1. Graham-Lorence, S., and Peterson, J. A. (1996) *FASEB J. 10*, 206−214.
2. Nelson, D. R., Kamataki, T., Waxman, D. J., Guengerich, F. P., Estabrook, R. W., Feyereisen, R., Gonzalez, F. J., Coon, M. J., Gunsalus, I. C., Gotoh, O., et al. (1993) *DNA Cell Biol. 12*, 1−51.
3. Rendic, S., and Di Carlo, F. J. (1997) *Drug Metab. Rev. 29*, 413−580.
4. Li, H., and Poulos, T. L. (1997) *Nat. Struct. Biol. 4*, 140−146.
5. Poulos, T. L., Finzel, B. C., and Howard, A. J. (1987) *J. Mol. Biol. 195*, 687−700.
6. Hasemann, C. A., Kurumbail, R. G., Boddupalli, S. S., Peterson, J. A., and Deisenhofer, J. (1995) *Structure 3*, 41−62.
7. Omura, T., and Sato, R. (1964) *J. Biol. Chem. 239*, 2370−2378.
8. Ravichandran, K. G., Boddupalli, S. S., Hasermann, C. A., Peterson, J. A., and Deisenhofer, J. (1993) *Science 261*, 731−736.
9. Hasemann, C. A., Ravichandran, K. G., Peterson, J. A., and Deisenhofer, J. (1994) *J. Mol. Biol. 236*, 1169−1185.
10. Boddupalli, S. S., Hasemann, C. A., Ravichandran, K. G., Lu, J. Y., Goldsmith, E. J., Deisenhofer, J., and Peterson, J. A. (1992) *Proc. Natl. Acad. Sci. U.S.A. 89*, 5567−5571.
11. Williams, P. A., Cosme, J., Sridhar, V., Johnson, E. F., and McRee, D. E. (2000) *Mol. Cell 5*, 121−131.
12. Zheng, Y. M., Fisher, M. B., Yokotani, N., Fujii-Kuriyama, Y., and Rettie, A. E. (1998) *Biochemistry 37*, 12847−12851.
13. Henne, K. R., Fisher, M. B., Iyer, K. R., Lang, D. H., Trager, W. F., and Rettie, A. E. (2001) *Biochemistry 40*, 8597−8605.
14. Hoch, U., and Ortiz de Montellano, P. R. (2001) *J. Biol. Chem. 276*, 11339−11346.
15. Haining, R. L., Hunter, A. P., Veronese, M. E., Trager, W. F., and Rettie, A. E. (1996) *Arch. Biochem. Biophys. 333*, 447−458.
16. Guan, X., Fisher, M. B., Lang, D. H., Zheng, Y. M., Koop, D. R., and Rettie, A. E. (1998) *Chem.-Biol. Interact. 110*, 103−121.
17. Laethem, R. M., Laethem, C. L., and Koop, D. R. (1992) *J. Biol. Chem. 267*, 5552−5559.
18. Christmas, P., Ursino, S. R., Fox, J. W., and Soberman, R. J. (1999) *J. Biol. Chem. 274*, 21191−21199.
19. Thomas, P. E., Ryan, D., and Levin, W. (1976) *Anal. Biochem. 75*, 168−176.
20. Romero, F. J., Ordonez, I., Arduini, A., and Cadenas, E. (1992) *J. Biol. Chem. 267*, 1680−1688.
21. Abu-Soud, H. M., Loftus, M., and Stuehr, D. J. (1995) *Biochemistry 34*, 11167−11175.
22. Andersson, L. A., Sono, M., and Dawson, J. H. (1983) *Biochim. Biophys. Acta 748*, 341−352.
23. Tomkova, A., Antalik, M., Bagel'ova, J., Miskovsky, P., and Ulicny, J. (1992) *Gen. Physiol. Biophys. 11*, 273−286.
24. Hrycay, E. G., and O'Brien, P. J. (1971) *Arch. Biochem. Biophys. 147*, 14−27.
25. Hrycay, E. G., and O'Brien, P. J. (1971) *Biochem. J. 125*, 12P.
26. Estabrook, R. W., Baron, J., Peterson, J., and Ishimura, Y. (1972) *Biochem. Soc. Symp. 34*, 159−185.
27. Berry, E. A., and Trumpower, B. L. (1987) *Anal. Biochem. 161*, 1−15.
28. Koenigs, L. L., Peter, R. M., Hunter, A. P., Haining, R. L., Rettie, A. E., Friedberg, T., Pritchard, M. P., Shou, M., Rushmore, T. H., and Trager, W. F. (1999) *Biochemistry 38*, 2312−2319.
29. Rae, T. D., and Goff, H. M. (1998) *J. Biol. Chem. 273*, 27968−27977.
30. Smith, K. M. (1975) in *Porphyrins and Metalloporphyrins* (Smith, K. M., Ed.) pp 381−398, Elsevier Scientific Publishing Co., Amsterdam.
31. White, R. E. (1991) *Pharmacol. Ther. 49*, 21−42.
32. Peterson, J. A., and Graham-Lorence, S. E. (1995) in *Cytochrome P450: Structure, Mechanism, and Biochemistry* (Ortiz de Montellano, P. R., Ed.) pp 151−180, Plenum Press, New York.
33. Yonetani, T. (1967) *J. Biol. Chem. 242*, 5008−5013.
34. Teale, F. W. J. (1959) *Biochim. Biophys. Acta 35*, 543.
35. Swanson, B. A., Halpert, J. R., Bornheim, L. M., and Ortiz de Montellano, P. R. (1992) *Arch. Biochem. Biophys. 292*, 42−46.
36. Swanson, B. A., Dutton, D. R., Lunetta, J. M., Yang, C. S., and Ortiz de Montellano, P. R. (1991) *J. Biol. Chem. 266*, 19258−19264.
37. Wagner, G. C., Perez, M., Toscano, W. A., Jr., and Gunsalus, I. C. (1981) *J. Biol. Chem. 256*, 6262−6265.
38. Fisher, M. B., Zheng, Y. M., and Rettie, A. E. (1998) *Biochem. Biophys. Res. Commun. 248*, 352−355.
39. Marnett, L. J., and Kennedy, T. A. (1995) in *Cytochrome P450: Structure, Mechanism, and Biochemistry* (Ortiz de Montellano, P. R., Ed.) pp 49−80, Plenum Press, New York.
40. Fenna, R., Zeng, J., and Davey, C. (1995) *Arch. Biochem. Biophys. 316*, 653−656.
41. DePillis, G. D., Ozaki, S., Kuo, J. M., Maltby, D. A., and Ortiz de Montellano, P. R. (1997) *J. Biol. Chem. 272*, 8857−8860.
42. Hashizume, T., Imaoka, S., Hiroi, T., Terauchi, Y., Fujii, T., Miyazaki, H., Kamataki, T., and Funae, Y. (2001) *Biochem. Biophys. Res. Commun. 280*, 1135−1141.
43. Bylund, J., Hidestrand, M., Ingelman-Sundberg, M., and Oliw, E. H. (2000) *J. Biol. Chem. 275*, 21844−21849.

BI011171Z